Developmental Cell
Article

A Morphologically Conserved Nonapoptotic Program Promotes Linker Cell Death in *Caenorhabditis elegans*

Mary C. Abraham,[1] Yun Lu,[1] and Shai Shaham[1,*]
[1] Laboratory of Developmental Genetics, The Rockefeller University, 1230 York Avenue, New York, NY 10021, USA
*Correspondence: shaham@rockefeller.edu
DOI 10.1016/j.devcel.2006.11.012

SUMMARY

Apoptosis, cell death characterized by stereotypical morphological features, requires caspase proteases. Nonapoptotic, caspase-independent cell death pathways have been postulated; however, little is known about their molecular constituents or in vivo functions. Here, we show that death of the *Caenorhabditis elegans* linker cell during development is independent of the *ced-3* caspase and all known cell death genes. The linker cell employs a cell-autonomous death program, and a previously undescribed engulfment program is required for its clearance. Dying linker cells display nonapoptotic features, including nuclear crenellation, absence of chromatin condensation, organelle swelling, and accumulation of cytoplasmic membrane-bound structures. Similar features are seen during developmental death of neurons in the vertebrate spinal cord and ciliary ganglia. Linker cell death is controlled by the microRNA *let-7* and Zn-finger protein LIN-29, components of the *C. elegans* developmental timing pathway. We propose that the program executing linker cell death is conserved and used during vertebrate development.

INTRODUCTION

Programmed cell death plays essential roles during metazoan development, and is used to sculpt organs and to control morphogenesis. Inappropriate cell death contributes to the organ damage that accompanies many human disease states, and a reduced capacity for cell death is thought to be essential for the development of most, if not all, tumors (Lowe et al., 2004). Two major classes of programmed cell death have been distinguished based on morphological criteria (Clarke, 1990). During apoptotic cellular degradation, chromatin condenses, cytoplasmic volume is reduced, and little change in intracellular organelle number or morphology is evident. In autophagic cell death, vesicular structures enclosing bulk cytoplasm and organelles accumulate. Such autophagosomes fuse with lysosomes, leading to rapid autodegradation of cellular content (Yorimitsu and Klionsky, 2005). It is unclear whether autophagy promotes cell death or is used in a final survival effort to recycle essential building blocks (Abraham and Shaham, 2004; Levine and Yuan, 2005). Apoptosis and, in some cases, autophagic cell death are dependent on caspase proteases to effect cellular demise (Abraham and Shaham, 2004; Lee and Baehrecke, 2001). These death-promoting proteases degrade a variety of cellular targets; however, the precise cellular mechanisms by which they promote cell death are still unknown.

Despite the seemingly universal importance of caspases for cell death, some evidence suggests that programmed cell death can sometimes proceed in the absence of caspase activity. For example, ligand binding to death-domain-containing receptors, such as Fas and TNFR, can promote cell death in culture even in the presence of the pancaspase inhibitor, zVAD.fmk (Holler et al., 2000; Matsumura et al., 2000; Schulze-Osthoff et al., 1994; Vercammen et al., 1998). Likewise, cultured cells derived from *Apaf-1*$^{-/-}$ mice die in response to overexpression of BH3-domain-only proteins, such as tBID, BIM, and BAD, even when cells are incubated with zVAD.fmk and lack detectable caspase activity (Cheng et al., 2001). Genetic studies also hint at the possible existence of caspase-independent cell death. For example, the normal death of motor neurons in the mouse spinal cord is independent of either caspase-3 or caspase-9 (Oppenheim et al., 2001). Nonetheless, because multiple caspase-encoding genes exist in vertebrates, and because inhibitors may not fully attenuate caspase activity, it remains possible that some or all of these deaths are still mediated by caspases.

In the nematode *Caenorhabditis elegans*, four caspase-related genes exist: *ced-3*, *csp-1*, *csp-2*, and *csp-3* (Shaham, 1998; Yuan et al., 1993); however, only *ced-3* seems to be required for programmed cell death (Abraham and Shaham, 2004; Yuan et al., 1993), and only *ced-3* and *csp-1* are proteolytically active (Shaham, 1998). The CSP-2 caspase lacks key active-site residues, and *csp-3* encodes only a C-terminal caspase domain, entirely lacking the active site (Shaham, 1998). In somatic cells, CED-3 caspase activity is controlled by a conserved pathway consisting of three proteins: EGL-1 (BH3-only),

CED-9 (Bcl-2-related), and CED-4 (Apaf-1). In living cells, CED-9 protein is thought to bind to and sequester CED-4, preventing activation of CED-3. EGL-1 is expressed in some cells destined to die, and can bind to CED-9, releasing CED-4 and allowing it to promote CED-3 activation (Metzstein et al., 1998). The EGL-1-related protein, CED-13, may act similarly in the *C. elegans* germ line (Schumacher et al., 2005).

Most *C. elegans* cells destined to die during development do so within 30 min after they are born (Sulston and Horvitz, 1977; Sulston et al., 1983). The onset of these deaths is thought to be controlled by transcriptional induction of *egl-1*, and relevant transcription factors responsive to lineage and chromosomal sex cues have been identified for eight such cells (Conradt and Horvitz, 1999; Ellis and Horvitz, 1991; Hoeppner et al., 2004; Liu et al., 2006; Metzstein et al., 1996; Metzstein and Horvitz, 1999; Thellmann et al., 2003). Three *C. elegans* cells that die during normal development live much longer than most cells fated to die. Little is known about the function or death of one of these cells, MSpppaaa, the sister cell of the somatic gonad precursor cell, Z1. However, the other two long-lived cells, the tail-spike cell and the male-specific linker cell, exhibit obvious differentiated features (Sulston et al., 1980, 1983). The onset of tail-spike cell death is regulated by transcriptional activation of the *ced-3* caspase, a previously unappreciated form of cell death timing control (C. Waase and S.S., unpublished data). Our studies of linker cell death are presented here.

The linker cell is born during the second larval stage (L2) in the central region of the animal, and proceeds to follow a stereotypical path of migration. As the cell migrates, it leads the extension of the male gonad behind it (Kimble and Hirsh, 1979; Sulston et al., 1980) (Figures 1A–1C). Upon completion of its migration, the linker cell is positioned between the gonad (vas deferens) and the cloacal tube that serves as an exit channel for sperm in the adult. It is thought that removal of the linker cell during or just after the L4/adult transition may subsequently facilitate fusion between the vas deferens and cloaca, connecting the male reproductive system to the exterior (Figures 1A and 1D–1F). The dying linker cell is engulfed by either the U.lp or U.rp epithelial cells (abbreviated U.l/rp here), which are often fused with their anterior sibling cells (Sulston et al., 1980).

RESULTS

Linker Cell Death Is Controlled by a Cell-Intrinsic Program

It has been reported that linker cell death may depend on a signal from its engulfing cell (Sulston et al., 1980). To test this hypothesis, we used a laser microbeam to ablate U, the U.l/rp grandparental precursor cell. Linker cell fate in operated animals containing a genomically integrated *lag-2* promoter::GFP transgene, expressed in the linker cell, was followed until 2 hr after the L4/adult transition. By this time, linker cells in wild-type animals have already died (e.g., see Table 1). In 18/18 operated animals and 17/18 mock-ablated animals, linker cell death occurred, as assessed by disappearance of GFP expression or appearance of a GFP-labeled cell corpse. These results suggest that linker cell death does not require the U.l/rp cells. To test whether other local cues might promote linker cell death, we examined linker cell death in *him-4* mutant males in which linker cell migration is abnormal and the cell often migrates only to the anterior of the animal (Vogel and Hedgecock, 2001). As shown in Table 1, the linker cell died in most animals observed, suggesting that linker cell death can occur cell autonomously. However, the cell did survive in 17% of animals examined 8 hr after the L4/adult molt. Furthermore, a dying linker cell corpse was still visible in 87% (n = 30) of *him-4* mutants 2 hr after the molt, while corpses at this stage were observed in only 13% (n = 30) of wild-type animals. These results suggest that a local signal from the cloacal area may increase the efficiency with which linker cell death or engulfment proceeds.

Developmental Timing Genes Control Linker Cell Death

Linker cell death occurs at a specific place and time in developing *C. elegans* males. Given that spatial cues may only partially regulate linker cell death, we considered whether developmental timing might also be used as a cue to initiate cell death. In *lin-29* mutants, some cell types, such as seam cells, in adult animals manifest L4 characteristics, suggesting that *lin-29* is required for developmental progression in these cells (Rougvie and Ambros, 1995). We examined linker cell survival in *lin-29*(*n333*) mutant males and found that linker cell death was blocked in about half of these animals. Specifically, 16/30 *lin-29*(*n333*) males that we scored possessed a healthy-looking linker cell at its normal position within 2 hr of the transition to the adult, and 12/30 animals that we scored possessed a healthy linker cell 4–8 hr after the transition (Table 1; Figure 2A). Even after 24 hr, 7/20 linker cells still survived in *lin-29*(*n333*) animals. Similar effects were seen in *lin-29*(*n836*) males and in males in which *lin-29* had been inactivated by RNA interference (RNAi) (Table 1).

To determine whether *lin-29* was required in the linker cell or in the engulfing cell to promote linker cell death, we examined GFP localization in males carrying a transgene containing 3.5 kb of *lin-29* promoter sequences fused to GFP. This transgene was strongly expressed in the linker cell and was not observed in any neighboring cells, including the U.l/rp cells (Figure 2B), consistent with previous studies of LIN-29 protein localization (Euling et al., 1999). These experiments suggest that *lin-29* may function within the linker cell to promote cell death, and support the model that at least part of the program leading to linker cell death is cell autonomous.

To confirm this idea, we examined rescue of inappropriate linker cell survival in *lin-29*(*n836*) mutants carrying an unstably transmitted extrachromosomal array of the wild-type *lin-29* gene (see Experimental Procedures). As expected, the linker cell died in 19/20 animals in which both the linker cell and the surrounding cells (including U.l/rp) received the wild-type *lin-29* gene. Similarly, the

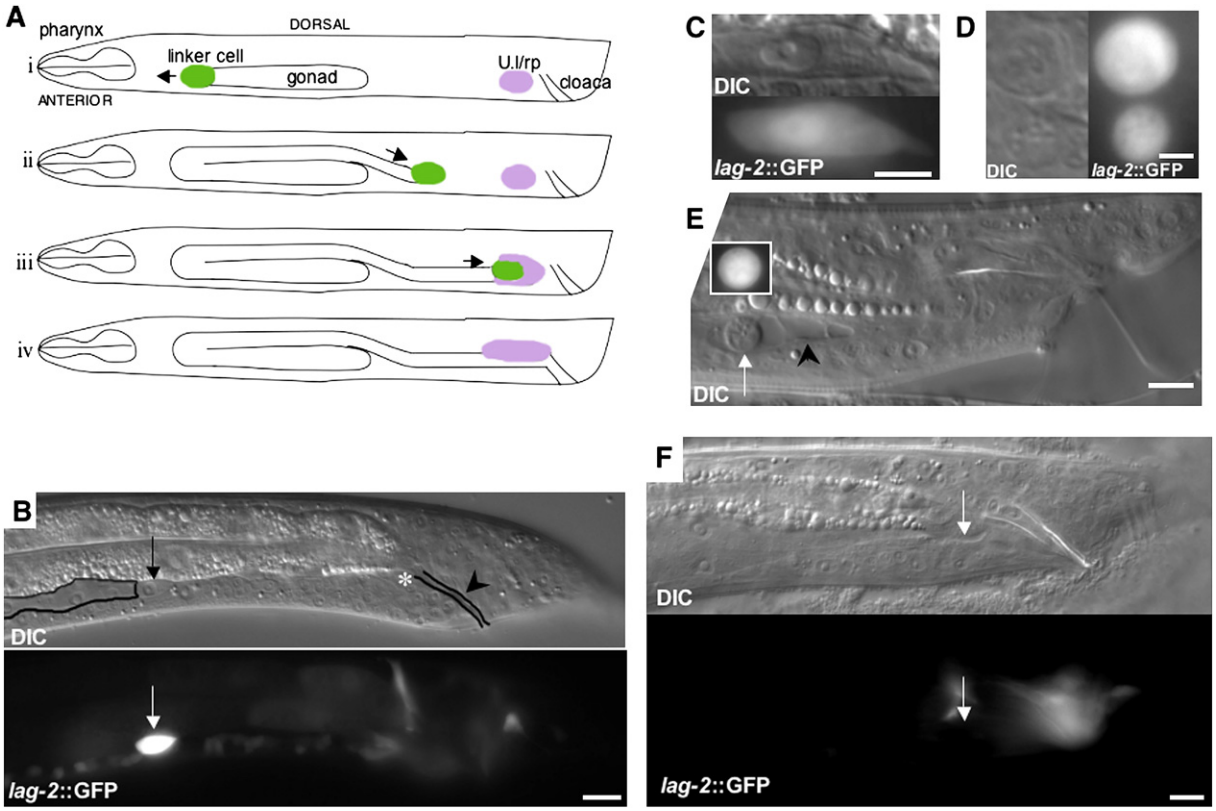

Figure 1. Linker Cell Death in Wild-Type Males

In all images in this paper, except Figure 3, anterior is to the left, dorsal is on top, and promoter::GFP and protein::GFP fusions are indicated as lowercase and uppercase letters, respectively.

(A) A diagram depicting stages of linker cell migration and death. (i) L2 animal; the linker cell has migrated anteriorly on the ventral side. (ii) Early-L4 animal; the linker cell is migrating posteriorly on the dorsal side. (iii) Late-L4 animal; the linker cell has reached the cloacal region, begins to die, and is engulfed by U.l/rp. (iv) Adult animal; the linker cell has died and disappeared. U.l/rp, which now has an extended morphology, connects to the vas deferens.

(B–F) Linker cell expressing a *lag-2* promoter::GFP transgene. (B, C, D, F) DIC (top in [B], [C], and [F] or left in [D]) and fluorescence (bottom in [B], [C], and [F] or right in [D]) images. (B) A healthy migrating linker cell at the L4 larval stage. Vas deferens is outlined in black, as is the cloaca (arrowhead). Arrow indicates linker cell. U.l/rp location is indicated with an asterisk. Scale bar, 10 μm. (C) A healthy migrating linker cell at the L3 stage. The nucleus is stained more brightly than the cell body. Note the prominent nucleolus within the nucleus. Scale bar, 2 μm. (D) A linker cell in a late-L4 stage animal undergoing cell death. Note that the cell has split into two parts. Scale bar, 1.5 μm. (E) A linker cell (arrow) in a late-L4 stage animal about to undergo the L4/adult molt. Inset, GFP expression in the linker cell. Note the characteristic roundness and refractility common to other programmed cell deaths in the animal. Arrowhead, a large vacuole within the U.l/rp engulfing cell (Figure S1). Vacuoles were not a result of prolonged incubation of the animal in sodium azide anesthetic, since they were visible immediately upon mounting for observation and could also be seen without anesthetic. Scale bar, 5 μm. (F) Young adult, less than 2 hr after L4/adult molt, in which the linker cell has died. Note the absence of GFP and absence of the linker cell in the region marked with an arrow. Scale bar, 10 μm.

linker cell died in 9/10 animals in which the linker cell received the wild-type *lin-29* gene but surrounding cells did not, supporting the notion that *lin-29* functions cell autonomously to regulate linker cell death. In agreement with this idea, the linker cell survived in 14/19 animals in which neither the linker cell nor the surrounding cells received the wild-type *lin-29* gene, and in 5/10 animals in which the linker cell lacked the wild-type *lin-29* gene but the surrounding cells had the gene (Figure 2C).

We also found that U.l/rp cells failed to extend phagocytic processes around the linker cell when the linker cell inappropriately survived in adult *lin-29* mutant males (compare Figure 2D and Figures 3A and 3B), even though U.l/rp still properly elongated, suggesting either that *lin-29* also regulates linker cell engulfment, or that initiation of *lin-29*-dependent linker cell death is a prerequisite for engulfment to occur.

lin-29 encodes a Zn-finger transcription factor, and is the most downstream known component of the pathway controlling developmental timing at the L4/adult transition in *C. elegans*. *lin-29* activity is inhibited by the *lin-41* gene, which in turn is inhibited by the microRNA *let-7* (Pasquinelli and Ruvkun, 2002; Reinhart et al., 2000; Slack et al., 2000). To determine whether *lin-29* functions within the linker cell in the context of the developmental timing program, we examined linker cell death in *let-7*(*n2853*) temperature-sensitive mutants. As shown in Table 1, at 25°C the linker cell inappropriately survived in these

Table 1. Effects of Mutations on Linker Cell Death

Genotype[a]	% Linker Cell Survival in 0–2-Hr-Old Adults (n)[b]	% Linker Cell Survival in 4–8-Hr-Old Adults (n)	No. Extra Cells in Anterior Pharynx (n)[c]
Wild-type	0 (30)	0 (30)	0.2 ± 0.4 (15)
him-4(*e1267*)	10 (30)	17 (30)	0.5 ± 0.8 (11)
him-4(RNAi)	13 (30)	17 (30)	0.3 ± 0.5 (10)
lin-29(*n333*)	53 (30)	40 (30)	0.3 ± 0.5 (12)
lin-29(*n836*)[d]	76 (21)	54 (13)	0.2 ± 0.4 (10)
lin-29(RNAi)[d]	50 (30), 52 (27)	24 (29), 48 (29)	0.2 ± 0.6 (15), 0.2 ± 0.4 (15)
let-7(*n2853*ts)[e]	20 (30)	17 (30)	0.2 ± 0.4 (15)
ced-1(*e1735*)	7 (30)	0 (29)	0.1 ± 0.3 (15)
ced-5(*n1812*)	3 (30)	0 (30)	0.3 ± 0.5 (15)
ced-7(*n1892*)	3 (30)	0 (30)	0.1 ± 0.3 (15)
ced-10(*n1993*)	0 (30)	3 (30)	0.3 ± 0.5 (15)
ced-1(*e1735*); *ced-5*(*n1812*)	3 (30)	3 (30)	0.1 ± 0.3 (10)
ced-7(*n1892*); *ced-10*(*n1993*)	0 (30)	3 (30)	0.3 ± 0.5 (13)
ced-3(*n717*)	0 (30)	0 (30)	10.5 ± 1.4 (15)
csp-1(*tm917*)	7 (30)	0 (30)	0.1 ± 0.4 (15)
csp-1(RNAi)	4 (26)	ND	ND
csp-2(*tm1079*)	3 (30)	3 (30)	0.1 ± 0.3 (15)
csp-3(RNAi)	7 (30)	0 (30)	0.1 ± 0.4 (15)
csp-1(*tm917*); *ced-3*(*n717*)	2 (50)	0 (30)	10.8 ± 1.7 (15)
HS-p35[f]	0 (31)	ND	3.9 ± 4.2 (14)
ced-4(*n1162*)	13 (30)	0 (30)	11.1 ± 1.4 (15)
ced-9(*n1950*)	16 (32)	0 (30)	10.9 ± 1.6 (10)
egl-1(*n1084n3082*)	3 (30)	3 (30)	10.6 ± 1.9 (10)
ced-13(*sv32*)	0 (30)	0 (30)	0.1 ± 0.4 (15)
ced-1(*e1735*); *ced-3*(*n717*)	0 (30)	0 (30)	10.8 ± 2.6 (15)
ced-2(*e1752*); *ced-3*(*n717*)	0 (30)	0 (30)	10.3 ± 1.4 (15)
ced-7(*n1892*); *ced-10*(*n1993*); *ced-3*(*n717*)[g]	18 (44)	15 (33)	10.3 ± 1.9 (15)
ced-1(*e1735*); *ced-4*(*n1162*); *ced-5*(*n1812*)	7 (30)	7 (30)	10.2 ± 1.3 (10)
ced-3(*n717*); *him-4*(*e1267*)	16 (32)	9 (32)	11.0 ± 1.4 (10)
ced-4(*n1162*); *him-4*(*e1267*)	16 (32)	3 (29)	9.9 ± 1.5 (10)
ced-7(*n1892*); *ced-10*(*n1993*); *ced-3*(*n717*); *him-4*(RNAi)[g]	38 (29)	29 (41)	10.2 ± 2.0 (15)
ced-1(*e1735*); *ced-4*(*n1162*); *ced-5*(*n1812*); *him-4*(RNAi)[h]	28 (29)	20 (30)	9.9 ± 1.7 (10)

n, number of animals scored. ND, not determined.

[a] All strains described, except for those containing *him-4*(*e1267*), also contained either the *him-5*(*e1467*) or *him-8*(*e1489*) mutations for high incidence of males. All strains also contained a genomically integrated *lag-2*::GFP linker cell reporter transgene. Strong loss-of-function alleles were used for all genes except *let-7*(*n2853*ts).

[b] Linker cell survival was assessed in populations of males allowed to grow for either 0–2 or 4–8 hr after the L4/adult molt, as described in the Experimental Procedures.

[c] Number of extra cells in the anterior pharynx of males of indicated genotype was assessed as described in the Experimental Procedures section. Mean ± SD.

[d] RNAi was performed with two different interfering constructs. In about 30% of *lin-29* mutants, the linker cell exhibited migration defects; however, we only scored males in which the linker cell reached the U.l/rp cell. The *lin-29*(*n836*) strain also contained the *unc-36*(*e251*) allele.

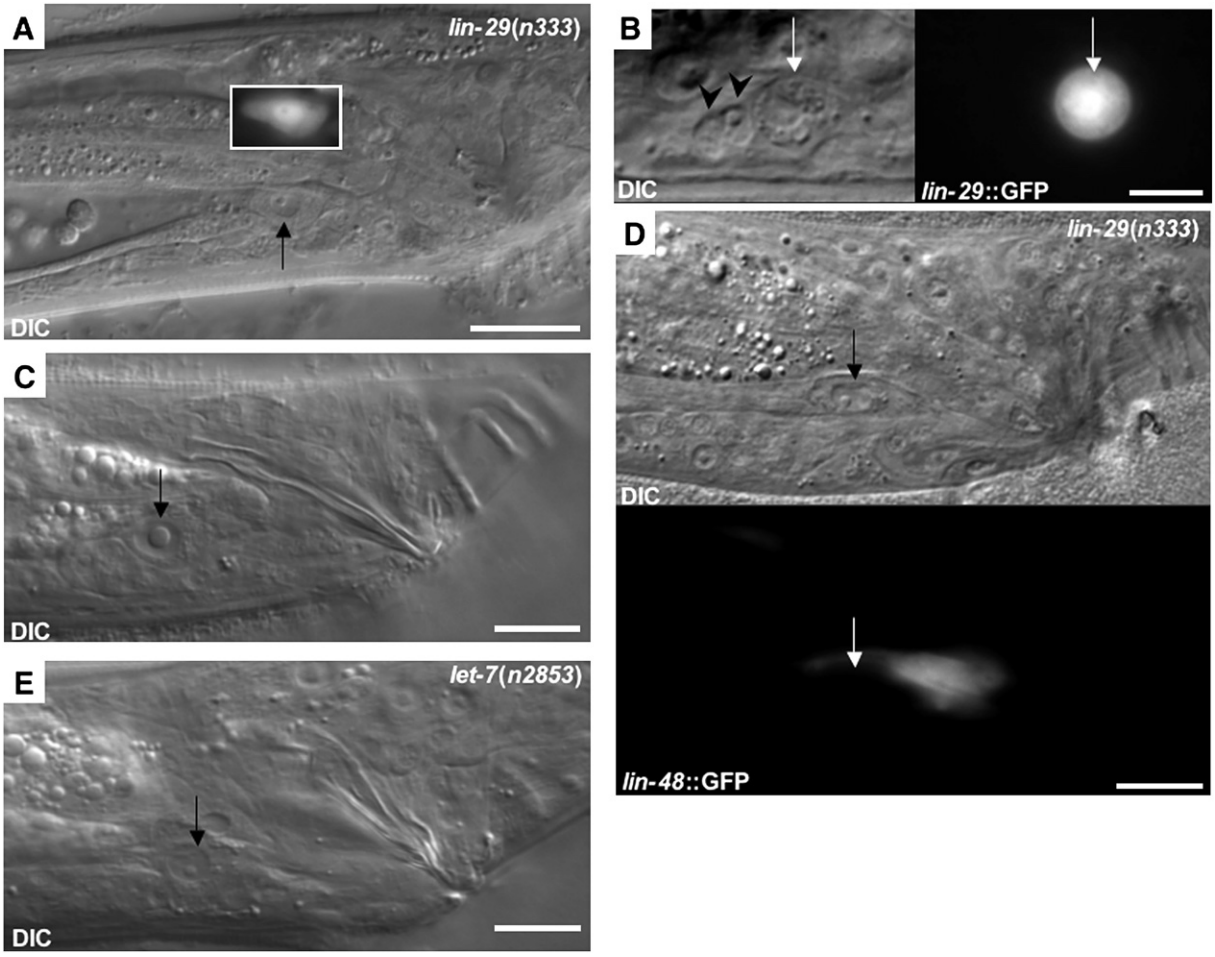

Figure 2. Linker Cell Death Is Regulated by Developmental Timing Genes

(A) A surviving linker cell in an 8-hr-old *lin-29*(*n333*) mutant adult. The linker cell (arrow) is marked with a *lag-2* promoter::GFP reporter (see inset). Scale bar, 10 μm.

(B) A transgene containing a 3.5 kb *lin-29* promoter fragment fused to GFP is expressed in the linker cell (arrow) at the L4 stage, but not in neighboring cells. Left, DIC image; right, fluorescence image. Arrowheads indicate engulfing cell nuclei. Scale bar, 5 μm.

(C) A surviving linker cell (arrow) in a mosaic animal that lacks *lin-29* in the linker cell (hence the prominent nucleolus), but has *lin-29* in neighboring cells. For details see text. Scale bar, 10 μm.

(D) A surviving linker cell (arrow) in a *lin-29*(*n333*) adult male is not engulfed by the U.l/rp cell. DIC (top) and fluorescence (bottom) images. The engulfing cell is marked with a *lin-48* promoter::GFP transgene. Note that obvious extensions encircling the linker cell are absent. Scale bar, 10 μm.

(E) A surviving linker cell (arrow) in a *let-7*(*n2853*) 7-hr-old adult. Scale bar, 10 μm.

mutants (Figure 2E). The extent of survival was lower than in *lin-29* mutants, presumably because *let-7*(*n2853*) mutants still retain some *let-7* function. This result supports the idea that linker cell death is regulated by the *C. elegans* developmental timing pathway.

Linker Cell Engulfment Is Independent of Known Engulfment Genes

Two partially redundant pathways have been described in *C. elegans* for the phagocytosis of both apoptotic (Gumienny and Hengartner, 2001; Mangahas and Zhou, 2005)

[e] *let-7*(*n2853*ts) animals were scored at 25°C; in wild-type animals, growth at 25°C had no effect on linker cell death (n = 30 for each time point).

[f] p35 expression was induced by applying a 45 min heat shock to L4 males, or early during embryogenesis, to assess pharyngeal cell survival.

[g] Unlike the other strains in this table, these strains were, for unknown reasons, particularly unhealthy, and grew very slowly. Therefore, any survival seen may reflect these developmental defects, preventing direct comparison with other strains in the table.

[h] The differences between this genotype and *him-4*(RNAi) were not statistically significant, with $p > 0.21$ for any pairwise data comparisons using Student's t test.

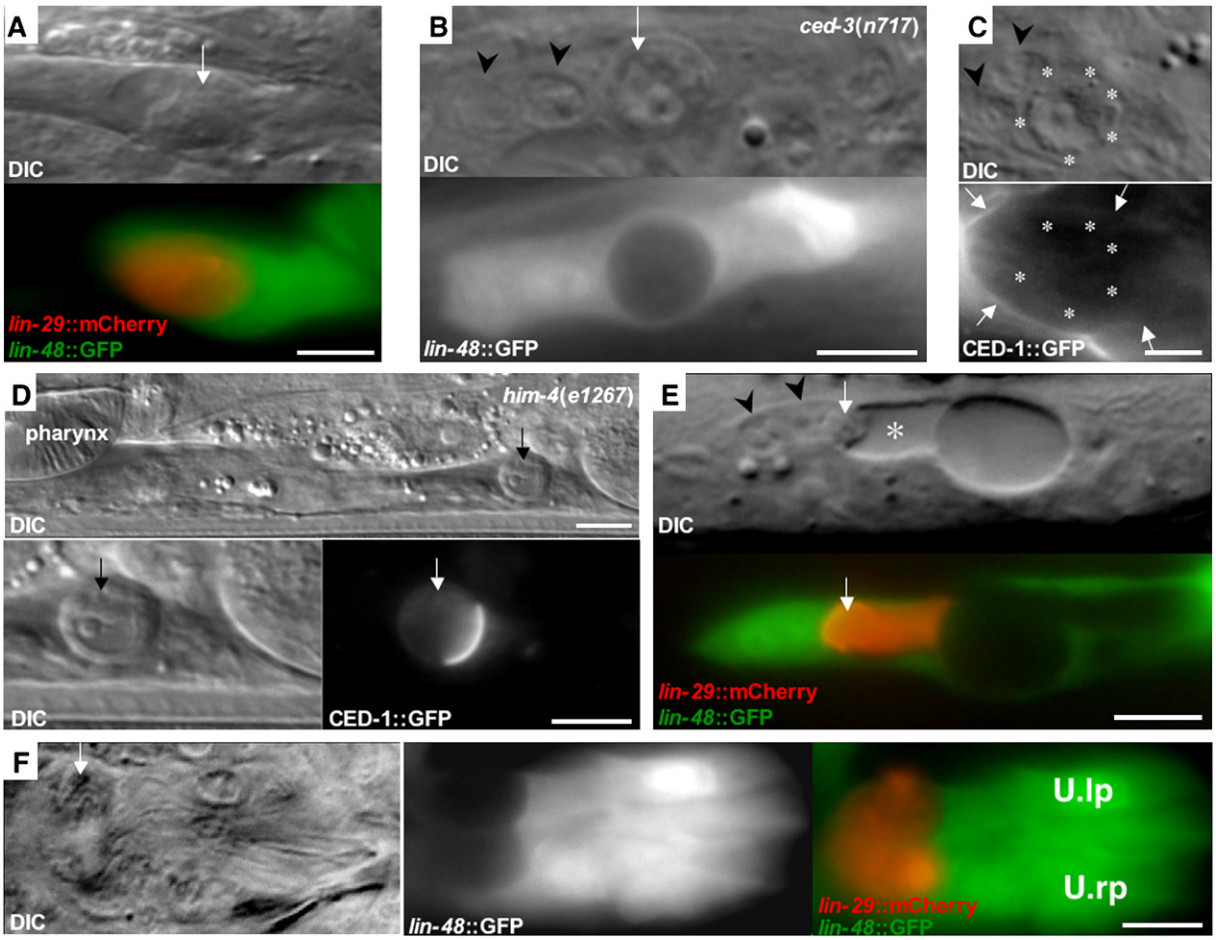

Figure 3. Linker Cell Engulfment in Wild-Type and Mutant Animals

(A) Linker cell (arrow) expressing a *lin-29* promoter::mCherry reporter transgene is engulfed by a U.l/rp cell expressing a *lin-48* promoter::GFP reporter transgene. Top, DIC image; bottom, fluorescence image. Scale bar, 5 μm.

(B) A dying and fully engulfed linker cell (arrow) in a *ced-3*(*n717*) male expressing a *lin-48* promoter::GFP reporter in the U.l/rp cell. Arrowheads, nuclei of engulfing cell. DIC (top) and fluorescence (bottom) images. Scale bar, 5 μm.

(C) A linker cell (outlined with asterisks) dying in its normal position does not induce CED-1::GFP clustering, even though CED-1::GFP is expressed on the engulfing cell membrane (arrows). Arrowheads, nuclei of engulfing cell. DIC (top) and fluorescence (bottom) images. Scale bar, 5 μm.

(D) Top: DIC image of a dying linker cell (arrow) in a *him-4*(*e1267*) male. Note that the cell has failed to complete its normal migration, and ends up in an anterior ventral position. Bottom: close-up DIC (left) and fluorescence (right) images of the linker cell showing linker cell engulfment by a neighboring cell expressing CED-1::GFP. Note GFP clustering around the linker cell. Scale bars, 5 μm.

(E) DIC (top) and fluorescence (bottom) images of a clear vacuole (asterisk) containing mCherry in an animal expressing *lin-29* promoter::mCherry (arrow, linker cell corpse) and *lin-48*::GFP (U.l/rp) transgenes late during linker cell death. Arrowheads, nuclei of engulfing cell. Scale bar, 5 μm.

(F) DIC (left), GFP fluorescence (middle), and combined GFP+mCherry fluorescence (right) images of a linker cell (arrow) expressing a *lin-29* promoter::mCherry reporter transgene being divided into two parts as it is being engulfed by U.lp (top cell) and U.rp (bottom cell) expressing a *lin-48* promoter::GFP reporter transgene. Scale bar, 5 μm.

and necrotic (Chung et al., 2000) cells. One pathway consists of the genes *ced-1*, *ced-6*, and *ced-7*, and the other of the genes *ced-2*, *ced-5*, *ced-10*, and *ced-12*. To assess whether engulfment contributes to linker cell demise, and to study linker cell engulfment, we examined linker cell survival in animals containing mutations in engulfment genes. We found that these mutations had no effect on survival (Table 1). For example, within a 2 hr period after the L4/adult transition, the linker cell died in 29/30 animals defective for both the *ced-1* and *ced-5* engulfment genes. These results suggest either that engulfment is not necessary for linker cell death, or that the known engulfment genes do not participate in linker cell engulfment, or both. To distinguish between these possibilities, we assessed the efficiency of linker cell engulfment by the U.l/rp cells in animals carrying mutations in known engulfment genes. Specifically, GFP-labeled U.l/rp cells of males undergoing the L4/adult molt were examined for cellular extensions completely surrounding the linker cell. Surprisingly, we found that engulfment still proceeded at high

Table 2. Mutants of Known Engulfment Genes Do Not Block Linker Cell Engulfment

Genotype	% U.l/rp Cells Extending Processes to Surround the Linker Cell (n)[a]
Wild-type	96 (27)
ced-1(*e1735*)	100 (30)
ced-5(*n1812*)	100 (30)
ced-7(*n1892*)	97 (30)
ced-10(*n1993*)	93 (30)
ced-10(*n3417*)[b]	92 (13)
dyn-1(*ky51*ts)[c]	100 (32)
ced-1(*e1735*); *ced-5*(*n1812*)	97 (31)

n, number of animals observed.
[a] Animals were scored at the late-L4 stage just prior to the molt to adult to provide enough time for complete engulfment, if it occurred, to become obvious.
[b] Homozygous mutants of this allele from a homozygous *ced-10* mother are embryonic lethal; therefore, we scored homozygous *ced-10* males from *ced-10*/+ mothers (homozygosity confirmed by PCR). Maternally rescued *ced-10* homozygotes are not embryonic lethal, but show engulfment defects at later stages of development (Kinchen et al., 2005).
[c] Animals shifted to the nonpermissive temperature (25°C) at least 12 hr prior to scoring.

efficiency in these mutants. For example, 30/31 linker cells were still engulfed in *ced-1*(*e1735*); *ced-5*(*n1812*) double mutants (Table 2). By comparison, the NSM-sister cell that dies during development is not engulfed in 52% of *ced-1*(*e1735*); *ced-5*(*n1812*) double mutants (Ellis et al., 1991), and the tail-spike cell is not engulfed in 94% of *ced-5*(*n1812*) mutants (C. Waase and S.S., unpublished data).

The CED-1 transmembrane protein is expressed in engulfing cells and clusters around dying cells to promote engulfment (Zhou et al., 2001). Consistent with our observation that mutants in the known engulfment pathway do not block linker cell engulfment, we never detected CED-1 clustering around the linker cell in wild-type animals, despite expression of the gene in U.l/rp cells (n = 30) (Figure 3C). Taken together, these results suggest that linker cell engulfment proceeds, at least in part, by a previously undescribed mechanism.

Does the linker cell require engulfment to die? We found that CED-1::GFP protein did cluster around and encircle the linker cell when the cell died at an abnormal location in a *him-4* mutant. However, at this location, morphological changes similar to those observed during normal linker cell death (see below; see also Figure S1 in the Supplemental Data available with this article online) preceded complete engulfment of the cell (Figure 3D). This observation suggests that the linker cell may initiate cell death prior to engulfment.

Linker Cell Death Is Independent of All Known Cell Death Genes

Although a dying linker cell resembles other dying cells in the animal when viewed using differential interference contrast (DIC) microscopy (Figure 1E), the dependence of this death on known *C. elegans* cell death genes has not been extensively studied. Ellis and Horvitz (1986) reported that linker cell death occurred in 3/5 *ced-3* mutant males, 2/6 *ced-4* mutant males, and 1/6 *ced-4*(*n1162*); *ced-3*(*n717*) males that they examined, suggesting that, while linker cell death was dependent on *ced-3* and *ced-4*, it could proceed in their absence. Surprisingly, we found that the linker cell died just after the L4/adult transition in 30/30 *ced-3*(*n717*) loss-of-function (lf) mutant males examined, suggesting that linker cell death was completely independent of *ced-3* (Table 1; Figure 3B). One possible reason for the stronger block in linker cell death that we observed may be that, in previous studies, the linker cell was not followed during and after the L4/adult molt (Ellis and Horvitz, 1986). Thus, scoring the state of the cell too early may have been misleading. Another possibility is that, after the transition to the adult, the linker cell becomes more difficult to distinguish from nearby cells. Therefore, we always used *lag-2*::GFP or *mig-24*::GFP reporter transgenes to facilitate scoring linker cell presence.

To examine whether other *C. elegans* caspases may be required for linker cell death, we assessed linker cell death in males with deletions in the *csp-1* and *csp-2* genes, or subjected to RNAi directed toward *csp-1* or *csp-3*. The *csp-1*(*tm917*) mutation is a 749 bp deletion in sequences encoding the N-terminal noncatalytic domain of the protein. The *csp-2*(*tm1079*) mutation consists of a 680 bp deletion in sequences encoding the N-terminal noncatalytic domain of the protein and a duplication of a small portion of this domain. As shown in Table 1, none of these mutants affected linker cell death. Furthermore, linker cell death still occurred in *csp-1*; *ced-3* double mutants, and in males in which the caspase inhibitor, p35, was overexpressed using a heat shock promoter (Sugimoto et al., 1994). Taken together, these data suggest that linker cell death is *ced-3*-independent and likely caspase-independent.

ced-3-independent but *ced-4*-dependent cell death has been previously reported in *C. elegans* embryos carrying mutations in the *icd-1* gene (Bloss et al., 2003). To determine whether linker cell death proceeded using a similar mechanism, we examined linker cell death in *ced-4*(lf) mutants. We found that linker cell death still occurred within 4–8 hr of the L4/adult transition in 30/30 *ced-4*(*n1162*) males that we examined (Table 1). Likewise, linker cell death still occurred in males carrying an *egl-1*(lf) mutation or a *ced-9*(*n1950*) gain-of-function mutation, both of which prevent the deaths of most somatic *C. elegans* cells destined to die (Conradt and Horvitz, 1998; Hengartner et al., 1992) (Table 1). Furthermore, linker cell death still occurred in the large majority of animals carrying combinations of mutations in *ced-3*, *ced-4*, *him-4*, and the engulfment-promoting genes *ced-1*, *ced-2*, *ced-5*, *ced-7*, and *ced-10* (Table 1), demonstrating that, even in these highly sensitized genetic backgrounds, linker cell death

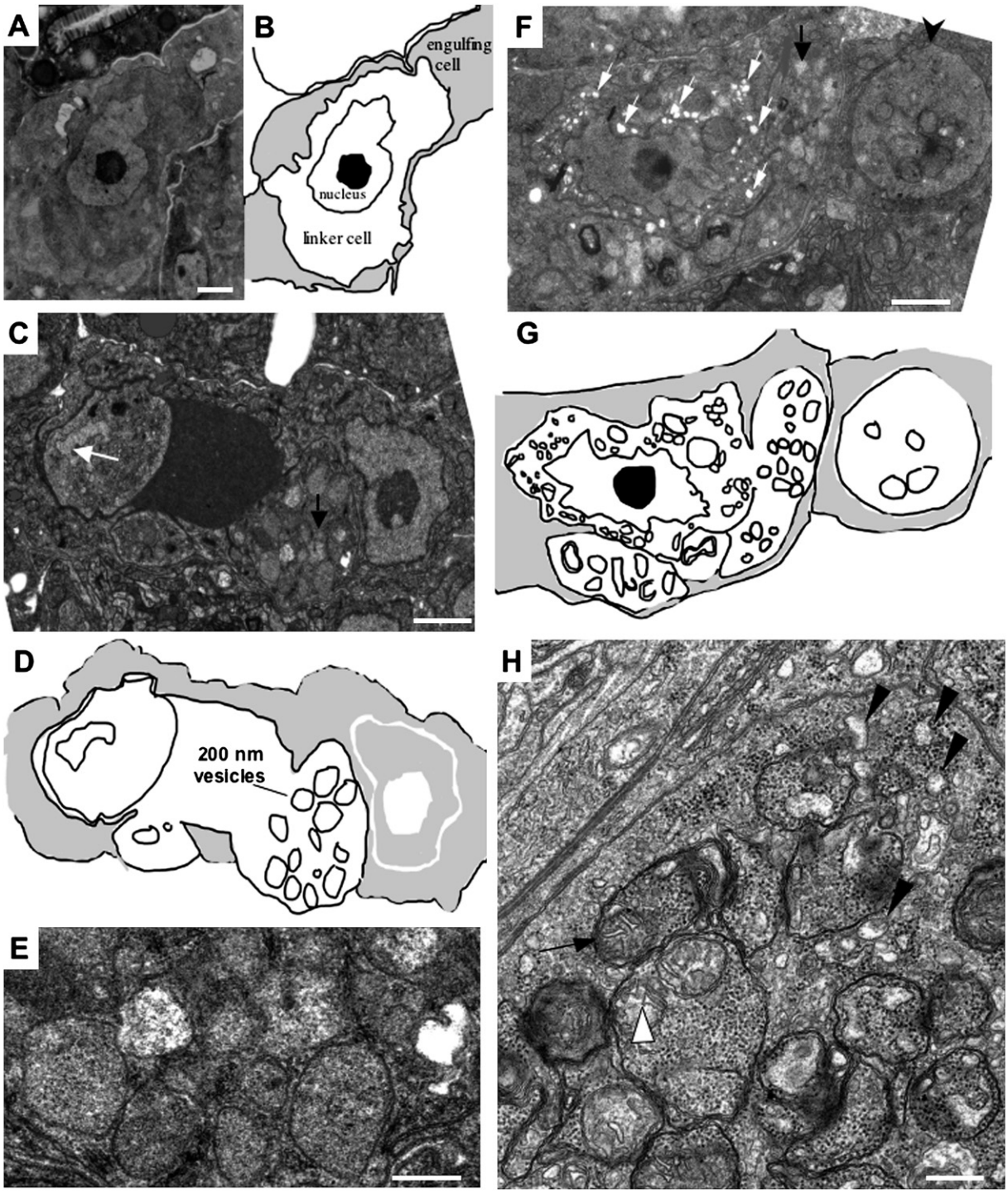

Figure 4. Linker Cell Death Is Not Apoptotic

(A) Image of a linker cell at the beginning of the cell death process before an obvious corpse structure is seen by DIC microscopy. Note that, although engulfed, the linker cell displays normal morphology, including a well-defined nucleus and a prominent nucleolus (black circular structure). Scale bar, 1 μm.

(B) A tracing of image in (A).

(C) A linker cell at a later stage of death. Note the accumulation of 200 nm vesicles (black arrow), possibly degraded mitochondria, within the linker cell. Note absence of condensed chromatin in the nucleus (white arrow). The darkly staining material in the middle of the cell was only seen in 1/11 linker cells that we examined. Scale bar, 1 μm.

(D) A tracing of image in (C).

could proceed efficiently. Although a slight delay in linker cell death occurred in *ced-4*(*n1162*) and *ced-9*(*n1950*) mutants (Table 1), this delay was not statistically significant, and may be attributable to a slight developmental delay in these mutants, rather than a direct effect on linker cell death per se. Taken together, the results presented here suggest that linker cell death must be regulated, at least in part, by a previously undescribed cell death program.

Linker Cell Death Morphology Is Not Apoptotic, but Is Conserved

Our findings that genes mediating apoptosis were not required for linker cell death strongly suggested that linker cell death may be very different from apoptosis, despite the similarities to apoptotic deaths observed using DIC microscopy (Figure 1E). To test this idea, we examined linker cells at different stages of death using fluorescence and electron microscopy (EM). As shown in Figure 4, we found that dying linker cells did not display characteristic apoptotic features. The linker cell is engulfed by the U.l/rp cell early in the death process (Figures 4A and 4B), and, although engulfed, the cell looks healthy, retaining well-defined nuclear, nucleolar, and cytoplasmic structures. Later, the cell exhibits increased indentation (crenellation) of the nucleus in the absence of chromatin compaction (Figures 4C, 4D, 4F, and 4G, and Figure S1A), and formation and aggregation of 200 nm wide single-membrane cytoplasmic vesicles (Figures 4C–4E), some of which may be swollen mitochondria. Swollen and degraded mitochondria within large multilayered membrane-bound structures could also be clearly seen (Figure 4H), and small electron-translucent "empty" membrane-bound cytoplasmic structures were abundant during linker cell death (Figures 4F–4H). Vacuoles resembling structures seen during necrotic cell death in *C. elegans* (Hall et al., 1997) could be seen at later stages within the U.l/rp cell (Figures 1E and 3E, and Figure S1B). Some of these vacuoles clearly contained material derived from the linker cell (Figure 3E). However, reducing the functions of the proteases *clp-1*, *tra-3*, *asp-3*, or *asp-4*, which promote the necrotic morphology of *C. elegans* neurons expressing the constitutively open DEG/ENaC channel MEC-4 (Syntichaki et al., 2002; Xu et al., 2000), did not affect linker cell death (Table 3), suggesting that the program promoting linker cell death differs, at least in some respects, from MEC-4-induced necrosis. Finally, by fluorescence microscopy, we often noticed that dying linker cells, marked with GFP or mCherry reporters, split into two bodies engulfed separately by U.lp and U.rp (Figures 1D and 3F). This observation was confirmed by EM (Figures 4F and 4G).

Table 3. Autophagy, Necrosis, or Wallerian Degeneration Mutants Do Not Block Linker Cell Death

Genotype	% Linker Cell Survival (n)[a]
bec-1(*ok700*)	0 (20)
unc-51(*e369*)	0 (19)
clp-1(RNAi)[b]	0 (22)
tra-3(RNAi)	0 (22)
asp-3(RNAi)	0 (23)
asp-4(RNAi)	0 (23)
Wld^S expression[c]	0 (60)

n, number of animals observed.
[a] Animals were scored 2–4 hr after the L4/adult molt, as described in Table 1, apart from the *bec-1* animals, which die at late L4, and were scored just around the molt to adult.
[b] RNAi was performed as described in Experimental Procedures.
[c] Expression driven from the *mig-24* promoter; results are combined data from three independent transgenic lines observed.

The accumulation of vesicles within the linker cell raised the possibility that these may be autophagosomes, However, three observations argue against this view. First, at least some of the vesicles that we observed were morphologically distinct from previously described autophagosomes (Baehrecke, 2003, 2005; Levine and Yuan, 2005), since they contained either single or several membranous layers (e.g., Figure 4H). Second, we examined expression of an LGG-1::GFP protein, a marker for autophagosomal membranes (Melendez et al., 2003; Roudier et al., 2005), in the linker cell. LGG-1::GFP puncta could be seen in migrating linker cells; however, their abundance only increased by about 1.5-fold as the cells proceeded to die (Figure S2). Third, we followed linker cell death in animals carrying mutations in the *bec-1* and *unc-51* genes, homologs of the autophagy genes beclin (Melendez et al., 2003; Takacs-Vellai et al., 2005) and APG1 (Matsuura et al., 1997), respectively. We saw no effects on linker cell survival in these mutants (Table 3). Taken together, these results suggest that autophagy does not play a major role in linker cell death.

Although programmed cell death has been frequently classified as either apoptotic or autophagic, Clarke (1990) previously defined a third class of cell death, characterized predominantly by cytoplasmic changes, that exhibits striking morphological similarities to linker cell death. This form of cell death involves nuclear crenellation

(E) The vesicles shown in (C) at higher magnification. Scale bar, 100 nm.
(F) Another linker cell at a late stage of death. The nuclear envelope is crenellated (indented). Black arrow indicates 200 nm vesicles. Arrowhead, a large membrane-bound structure that may correspond to the GFP-labeled bleb seen in Figure 1D. Note the "empty" clearings within the cytoplasm (white arrows). Scale bar, 1 μm.
(G) A tracing of image in (F).
(H) A late-stage dying linker cell. Note multilayered membrane structures surrounding mitochondria (arrow), the dilation of mitochondrial cristae (white arrowhead), and small clearings in the cytoplasm (black arrowheads). Scale bar, 200 nm.

(indentation) in the absence of chromatin compaction, accompanied by cytoplasmic changes characterized by "dilation of ER, nuclear envelope, Golgi and sometimes mitochondria, forming 'empty' spaces" (Clarke, 1990). Several researchers have reported observing cell death with similar features in vertebrates. For example, Pilar and Landmesser (1976) described such morphological features during the normal death of neurons in developing chick ciliary ganglia. A similar morphology was described in chick retinal ganglion cells that have been axotomized (Borsello et al., 2002), and in motor neurons that normally die in the chick spinal cord (Chu-Wang and Oppenheim, 1978). Intriguingly, spinal motor neurons in mice lacking caspase-3 or caspase-9 die as in normal development, and display mitochondrial swelling and electron-translucent cytoplasmic structures similar to those seen in dying linker cells (Oppenheim et al., 2001).

Taken together, our EM studies suggest that linker cell death involves a morphologically distinct form of programmed cell death that may be conserved in vertebrates.

It is of note that some of the conserved morphological features characterizing linker cell death, such as mitochondrial swelling and clustering, and the appearance of "empty" cytoplasmic membrane-bound structures, are also seen in Wallerian degeneration of axons (Griffin et al., 1996; Raff et al., 2002; Vial, 1958; Webster, 1962). This caspase-independent degenerative program occurs after axon transection, and may be used for normal pruning that takes place in the developing nervous system. Thus, molecular components promoting this form of cytoplasmic degeneration may be similar to those promoting linker cell death. However, expression of the Wallerian degeneration inhibitor gene Wld^s in the linker cell failed to prevent linker cell death (Table 3). This suggests that linker cell death employs a program distinct, at least in part, from Wallerian degeneration, although we were unable to monitor directly the levels of Wld^s expression.

DISCUSSION

Linker cell death in *C. elegans* must be tightly regulated to ensure male fertility. Death of the linker cell prior to completion of its migration results in severe defects in gonadal elongation, as has been demonstrated by ablation of the linker cell during its migration (Kimble and White, 1981; M.A. and S.S., unpublished data). It has been postulated that, once the linker cell has completed its migration, cell death must ensue to allow fusion of the gonadal and cloacal tubes of the male. Our studies suggest that this may indeed be the case, since we have shown that, in *lin-29* and *let-7* mutants, the connection between these tubes fails to form, and sperm accumulate within the male reproductive system (compare Figure 1F and Figure S3).

The studies described here also suggest that, even though linker cell death is cell intrinsic, both spatial and developmental inputs contribute to the cell's demise. Specifically, proximity to the cloaca seems to promote efficient linker cell death, helping to ensure that the cell dies at the right place. The developmental timing pathway provides information ensuring that linker cell death occurs at the right developmental stage.

The developmental timing transcription factor *lin-29* promotes both linker cell death and engulfment. Several observations suggest that *lin-29* does not function as a general regulator of linker cell fate. In *lin-29*(*n333*) mutants, for example, the linker cell displays normal morphology, expresses the *lag-2* and *mig-24* genes appropriately, and can lead gonad migration. Although migration of the cell is defective in about 30% of animals (Euling et al., 1999; M.A. and S.S., unpublished data), the cell-death defect in these mutants is still evident in normally migrating linker cells (Table 1 and Table 1 footnotes). Thus, *lin-29* is likely to have specific roles during linker cell development, including, perhaps, transcription of genes promoting linker cell death and engulfment.

Although *lin-29* is required for linker cell death, it is probably not sufficient to promote cell death. The gene is normally expressed in other cells that do not die, and is expressed within the linker cell itself during the L3 and early L4 stages when the cell is still migrating (Euling et al., 1999; data not shown). These observations suggest that additional genes must exist that cooperate with *lin-29* to promote linker cell death.

Our results suggest that linker cell death is governed by a nonapoptotic cell-death program that is independent of all previously described *C. elegans* cell-death genes. Why might a different cell-death pathway be required in the linker cell? One possibility is that the linker cell is much larger than all other cells undergoing programmed cell death in the animal. Thus, apoptosis may not be the most efficient method to eliminate the cell. Indeed, the death of the large *Drosophila* salivary gland cells, although caspase-dependent, also seems to employ autophagy to help eliminate bulk cytoplasm (Baehrecke, 2003). Another possibility is that components of the dying linker cell are recycled in a way that is not possible under apoptotic conditions. For example, the large vesicles accumulating within the linker cell and taken up by U.l/rp may serve roles in the subsequent elongation of the U.l/rp cell and its attachment to the vas deferens (see Figure 1A). Yet another possibility is that lineage-specific constraints on gene expression may prevent expression of apoptotic genes in the linker cell, necessitating use of an alternative program.

Our results also suggest that engulfment of the linker cell is likely to be governed by an alternate program. Why is this so? In animals in which the linker cell fails to migrate normally, the linker cell corpse can end up within the male gonad (Figure S4). The presence of such a large body within the gonad may block sperm exit, even if the gonad and cloaca were able to fuse. The mode of engulfment used by the U.l/rp cell may be the most efficient means to ensure that the linker cell will not enter the gonad.

The morphological similarities between dying linker cells and dying vertebrate spinal cord motor neurons and ciliary ganglion cells are striking, and suggest that the molecular components executing linker cell death

may be conserved. Circumstantial evidence is consistent with the existence of an alternative vertebrate developmental cell death program. For example, despite the pervasiveness of programmed cell death during early murine development, none of the mutations known to affect cell death in the mouse block the gross progress of development, and in many cases, mutant mice live to birth or beyond (Honarpour et al., 2000). Furthermore, mutations in caspase-3 and casapse-9, which play important roles in apoptotic cell deaths in mice, do not block motor-neuron death in the developing spinal cord (Oppenheim et al., 2001). In addition, none of the mutations affecting cell death in the mouse seem to affect the total number of cells in the immune system to an extent that might be predicted given the large numbers of cells eliminated during normal T and B cell development. Finally, it has been previously demonstrated that the death of interdigital cells during murine development can proceed in the absence of Apaf-1 with a necrotic morphology (Chautan et al., 1999). Although all of these examples could be explained by feedback control of cell numbers, and/or redundancy within caspase and other cell-death gene families, it is also possible that these cell deaths are regulated by an entirely different pathway similar to the one regulating linker cell death. If this is the case, this alternative mode of cell death must, therefore, play a major role during normal vertebrate development.

Evidence that linker cell death employs a conserved program may emerge from identification of the genes regulating this process. To identify such genes, we have performed a pilot genetic screen, seeking mutants in which the linker cell survives inappropriately. We identified five mutants in which the linker cell can survive. None of these mutants affected other programmed cell deaths that we examined (M.A. and S.S., unpublished data). These results are consistent with the evidence presented here demonstrating that linker cell death employs a novel cell death program. Further study of the mutants that we have identified may yield clues as to the molecular nature of linker cell death.

EXPERIMENTAL PROCEDURES

Strains and Alleles

Strains were handled using standard methods (Brenner, 1974). All strains were maintained and scored at 20°C unless otherwise indicated. Most strains included mutations promoting a high incidence of males (*him-4*(*e1267*), *him-5*(*e1467*, *e1490*), *him-8*(*e1489*)) as indicated. Alleles used in this study were described in the indicated references (alleles first reported here are unreferenced). Linkage group (LG) I: *ced-1(e1735)* (Hedgecock et al., 1983); LG II: *lin-29*(*n333*, *n836*) (Ambros and Horvitz, 1984), *csp-1*(*tm917*); LG III: *ced-4*(*n1162*) (Ellis and Horvitz, 1986), *ncl-1*(*e1865*) (Wood 1988), *unc-36*(*e251*) (Brenner, 1974), *ced-7*(*n1892*) (Ellis et al., 1991), *ced-9*(*n1950*) (Hengartner et al., 1992); LG IV: *ced-2*(*e1752*) (Ellis et al., 1991), *ced-10*(*n1993*) (Ellis et al., 1991), *ced-10 (n3417)* (Lundquist et al., 2001), *bec-1*(*ok700*) (Takacs-Vellai et al., 2005), *csp-2*(*tm1079*), *ced-5*(*n1812*) (Ellis et al., 1991), *him-8*(*e1489*) (Hodgkin and Brenner, 1977), *ced-3*(*n717*) (Ellis and Horvitz, 1986); LG V: *egl-1*(*n1084n3082*) (Conradt and Horvitz, 1998), *him-5*(*e1467*, *e1490*) (Hodgkin and Brenner, 1977), *unc-51*(*e369*) (Brenner, 1974); LGX: *ced-13*(*sv32*) (Schumacher et al., 2005), *him-4*(*e1267*) (Hodgkin and Brenner, 1977), *let-7*(*n2853*) (Reinhart et al., 2000), *dyn-1*(*ky51*) (Clark et al., 1997). *nT1 qIs51* (Belfiore et al., 2002) IV; V was used as a balancer for *bec-1*(*ok700*). Integrated transgenes used were: *qIs56* [*lag-2* promoter::GFP] (Siegfried and Kimble, 2002), *enIs7* [*ced-1* promoter::*ced-1*::GFP + *unc-76*(+)] (gift from Z. Zhou), *nsIs1* [*lag-2* promoter::GFP], *nsIs65* [*mig-24* promoter::GFP], *adIs2122* [*lgg-1* promoter::*lgg-1*::GFP + *rol-6*(*su1006*)] (gift from L. Avery), and *saIs14* [*lin-48* promoter::GFP] (gift from H. Chamberlin). The following extrachromosomal arrays were used: *nEx1049* [*ced-1* promoter::*ced-1*::GFP + *unc-76*(+)] (gift from Z. Zhou), *nsEx1265* [*lin-29* promoter::mCherry + *rol-6(su1006)*], *nsEx905-908* [*lin-29* promoter::GFP + *rol-6(su1006)*], *nsEx2000-2002* [*mig-24* promoter::Wld^S + *rol-6*(*su1006*)], *wEx15* [Heat-shock promoter::p35 + *rol-6*(*su1006*)] (Sugimoto et al., 1994), and *vEx112* [*lin-29*(+) *ncl-1*(+) *unc-36*(+)] (Euling et al., 1999).

U Cell Ablation Experiments

lin-48 promoter::GFP-marked U cells were ablated in L1 animals anaesthetized in a drop of M9 on 5% agar pads containing 5 mM sodium azide using standard methods (Bargmann and Avery, 1995). Ablations were scored as successful if, on the following day, the U cell was absent as observed by DIC and fluorescence microscopy. Mock-ablated animals provided controls. The strain used for ablation contained a *lag-2* promoter::GFP-marked linker cell to facilitate scoring of linker cell fate.

Mosaic Analysis

Mosaic analysis was carried out by scoring animals of the genotype *lin-29*(*n836*); *ncl-1*(*e1865*) *unc-36*(*e251*); *qIs56 him-5*(*e1490*) for loss of the extrachromosomal array, *vEx112*, containing *lin-29*(+), *ncl-1*(+), and *unc-36*(+). *unc-36* loss in the AB.p lineage, which gives rise to all the proctodeal cells that are in the vicinity of the linker cell at the time of its death (including the U.l/rp cells), confers an uncoordinated mobility phenotype. *unc-36* loss in the P1 lineage, giving rise to the linker cell, does not affect mobility. *ncl-1* loss results in large nucleoli. Mobility was assessed in L4 animals to determine whether array loss had occurred in the AB.p lineage. Animals were then mounted in S-Basal medium, and nucleolar size was used to confirm the presence or absence of the array in the U.l/rp and neighboring cells, and to determine if the array was present in the linker cell. Subsequent survival of the linker cell was followed in individual animals to determine whether the linker cell died, and whether death proceeded with normal kinetics. Only animals in which the linker cell migrated correctly were scored.

RNAi Assays

RNAi was carried out by feeding bacteria, expressing double-stranded RNA (dsRNA) corresponding to the gene of interest, to animals (Timmons and Fire, 1998). Plasmids used were obtained from the Ahringer library (Fraser et al., 2000), apart from the *csp-1* plasmid, which was from Open Biosystems. A synchronous population of L1 larvae was obtained by hypochlorite treatment, and animals were added to plates containing bacteria expressing dsRNA. Induction of dsRNA expression preceded the addition of animals to plates by 2–12 hr. Treated animals were scored upon reaching the L4/adult stage. An empty vector was used as a control.

Plasmid Constructions and Germline Transformation

Germline injections were used to create extrachromosomal arrays (Mello et al., 1991): 3.5 kb of the *lin-29* promoter was fused to GFP or mCherry and injected at 20 ng/μl with the *rol-6*(*su1006*) coinjection marker; 1 kb of the *mig-24* promoter was fused to Wld^S and injected at 10 ng/μl with the *rol-6*(*su1006*) coinjection marker.

Scoring Cell Survival

Extra cells in the anterior pharynx were scored by DIC microscopy at the L3 or L4 stage in males (Ellis and Horvitz, 1991). Linker cell death was recorded if both fluorescence and DIC microscopy revealed either the complete absence of the GFP-marked linker cell, or a linker cell

with a corpse morphology showing characteristics such as cell rounding, volume reduction, nuclear envelope breakdown, or large-scale blebbing.

EM

12 animals with a linker cell GFP marker were observed under a fluorescence dissecting microscope or by DIC microscopy to determine the approximate stage of linker cell death. Animals were then fixed, stained, embedded in resin, and serially sectioned using standard methods (Lundquist et al., 2001). Photographs were taken with an FEI Tecnai G2 Spirit BioTwin transmission electron microscope equipped with a Gatan 4K × 4K digital camera.

Supplemental Data

Supplemental Data, including supplemental figures, are available online at http://www.developmentalcell.com/cgi/content/full/12/1/73/DC1/.

ACKNOWLEDGMENTS

We thank Judith Kimble for the *lag-2*::GFP strain, Kiyoji Nishiwaki for the *mig-24*::GFP strain, Roger Tsien for the mCherry construct, Ann Rougvie for the *lin-29* mosaic strain, Helen Chamberlin for the *lin-48*::GFP strain, Zheng Zhou for the CED-1::GFP strain, Joel Rothman for the HS-p35 strain, Bob Horvitz for the *ced-10(n3417)* strain, Cori Bargmann for the *dyn-1(ky51)* strain, Michael Coleman for the Wld^S-containing plasmid, Leon Avery for the LGG-1::GFP strain, Shohei Mitani for the *csp-1*(*tm917*) and *csp-2*(*tm1079*) mutants, John Sulston for sharing unpublished information, Dave Hall for comments on some electron micrographs, and members of the Shaham laboratory for insightful comments on the manuscript. The studies presented here were supported by grants from the Irma T. Hirschl/Monique Weill-Caulier Trust, The Breast Cancer Alliance, and the National Institutes of Health (NIH) (S.S.). M.C.A. is a David Rockefeller fellow. S.S. is a Rita Allen fellow and a Klingenstein fellow in the neurosciences. Some nematode strains used in this work were provided by the *Caenorhabditis* Genetics Center, which is funded by the NIH National Center for Research Resources.

Received: July 20, 2006
Revised: November 1, 2006
Accepted: November 16, 2006
Published: January 8, 2007

REFERENCES

Abraham, M.C., and Shaham, S. (2004). Death without caspases, caspases without death. Trends Cell Biol. *14*, 184–193.

Ambros, V., and Horvitz, H.R. (1984). Heterochronic mutants of the nematode *Caenorhabditis elegans*. Science *226*, 409–416.

Baehrecke, E.H. (2003). Autophagic programmed cell death in *Drosophila*. Cell Death Differ. *10*, 940–945.

Baehrecke, E.H. (2005). Autophagy: dual roles in life and death? Nat. Rev. Mol. Cell Biol. *6*, 505–510.

Bargmann, C.I., and Avery, L. (1995). Laser killing of cells in *Caenorhabditis elegans*. Methods Cell Biol. *48*, 225–250.

Belfiore, M., Mathies, L.D., Pugnale, P., Moulder, G., Barstead, R., Kimble, J., and Puoti, A. (2002). The MEP-1 zinc-finger protein acts with MOG DEAH box proteins to control gene expression via the fem-3 3′ untranslated region in *Caenorhabditis elegans*. RNA *8*, 725–739.

Bloss, T.A., Witze, E.S., and Rothman, J.H. (2003). Suppression of CED-3-independent apoptosis by mitochondrial betaNAC in *Caenorhabditis elegans*. Nature *424*, 1066–1071.

Borsello, T., Mottier, V., Castagne, V., and Clarke, P.G. (2002). Ultrastructure of retinal ganglion cell death after axotomy in chick embryos. J. Comp. Neurol. *453*, 361–371.

Brenner, S. (1974). The genetics of *Caenorhabditis elegans*. Genetics *77*, 71–94.

Chautan, M., Chazal, G., Cecconi, F., Gruss, P., and Goldstein, P. (1999). Interdigital cell death can occur through a necrotic and caspase-independent pathway. Curr. Biol. *9*, 967–970.

Cheng, E.H., Wei, M.C., Weiler, S., Flavell, R.A., Mak, T.W., Lindsten, T., and Korsmeyer, S.J. (2001). BCL-2, BCL-X(L) sequester BH3 domain-only molecules preventing BAX- and BAK-mediated mitochondrial apoptosis. Mol. Cell *8*, 705–711.

Chu-Wang, I.W., and Oppenheim, R.W. (1978). Cell death of motoneurons in the chick embryo spinal cord: I. A light and electron microscopic study of naturally occurring and induced cell loss during development. J. Comp. Neurol. *177*, 33–57.

Chung, S., Gumienny, T.L., Hengartner, M.O., and Driscoll, M. (2000). A common set of engulfment genes mediates removal of both apoptotic and necrotic cell corpses in *C. elegans*. Nat. Cell Biol. *2*, 931–937.

Clark, S.G., Shurland, D.L., Meyerowitz, E.M., Bargmann, C.I., and van der Bliek, A.M. (1997). A dynamin GTPase mutation causes a rapid and reversible temperature-inducible locomotion defect in *C. elegans*. Proc. Natl. Acad. Sci. USA *94*, 10438–10443.

Clarke, P.G. (1990). Developmental cell death: morphological diversity and multiple mechanisms. Anat. Embryol. (Berl.) *181*, 195–213.

Conradt, B., and Horvitz, H.R. (1998). The *C. elegans* protein EGL-1 is required for programmed cell death and interacts with the Bcl-2-like protein CED-9. Cell *93*, 519–529.

Conradt, B., and Horvitz, H.R. (1999). The TRA-1A sex determination protein of *C. elegans* regulates sexually dimorphic cell deaths by repressing the *egl-1* cell death activator gene. Cell *98*, 317–327.

Ellis, H.M., and Horvitz, H.R. (1986). Genetic control of programmed cell death in the nematode *C. elegans*. Cell *44*, 817–829.

Ellis, R.E., and Horvitz, H.R. (1991). Two *C. elegans* genes control the programmed deaths of specific cells in the pharynx. Development *112*, 591–603.

Ellis, R.E., Jacobson, D.M., and Horvitz, H.R. (1991). Genes required for the engulfment of cell corpses during programmed cell death in *Caenorhabditis elegans*. Genetics *129*, 79–94.

Euling, S., Bettinger, J.C., and Rougvie, A.E. (1999). The LIN-29 transcription factor is required for proper morphogenesis of the *Caenorhabditis elegans* male tail. Dev. Biol. *206*, 142–156.

Fraser, A.G., Kamath, R.S., Zipperlen, P., Martinez-Campos, M., Sohrmann, M., and Ahringer, J. (2000). Functional genomic analysis of *C. elegans* chromosome I by systematic RNA interference. Nature *408*, 325–330.

Griffin, J.W., George, E.B., and Chaudhry, V. (1996). Wallerian degeneration in peripheral nerve disease. Baillieres Clin. Neurol. *5*, 65–75.

Gumienny, T.L., and Hengartner, M.O. (2001). How the worm removes corpses: the nematode *C. elegans* as a model system to study engulfment. Cell Death Differ. *8*, 564–568.

Hall, D.H., Gu, G., Garcia-Anoveros, J., Gong, L., Chalfie, M., and Driscoll, M. (1997). Neuropathology of degenerative cell death in *Caenorhabditis elegans*. J. Neurosci. *17*, 1033–1045.

Hedgecock, E.M., Sulston, J.E., and Thomson, J.N. (1983). Mutations affecting programmed cell deaths in the nematode *Caenorhabditis elegans*. Science *220*, 1277–1279.

Hengartner, M.O., Ellis, R.E., and Horvitz, H.R. (1992). *Caenorhabditis elegans* gene *ced-9* protects cells from programmed cell death. Nature *356*, 494–499.

Hodgkin, J.A., and Brenner, S. (1977). Mutations causing transformation of sexual phenotype in the nematode *Caenorhabditis elegans*. Genetics *86*, 275–287.

Hoeppner, D.J., Spector, M.S., Ratliff, T.M., Kinchen, J.M., Granat, S., Lin, S.C., Bhusri, S.S., Conradt, B., Herman, M.A., and Hengartner, M.O. (2004). *eor-1* and *eor-2* are required for cell-specific apoptotic death in *C. elegans*. Dev. Biol. *274*, 125–138.

Holler, N., Zaru, R., Micheau, O., Thome, M., Attinger, A., Valitutti, S., Bodmer, J.L., Schneider, P., Seed, B., and Tschopp, J. (2000). Fas triggers an alternative, caspase-8-independent cell death pathway using the kinase RIP as effector molecule. Nat. Immunol. *1*, 489–495.

Honarpour, N., Du, C., Richardson, J.A., Hammer, R.E., Wang, X., and Herz, J. (2000). Adult Apaf-1-deficient mice exhibit male infertility. Dev. Biol. *218*, 248–258.

Kinchen, J.M., Cabello, J., Klingele, D., Wong, K., Feichtinger, R., Schnabel, H., Schnabel, R., and Hengartner, M.O. (2005). Two pathways converge at CED-10 to mediate actin rearrangement and corpse removal in *C. elegans*. Nature *434*, 93–99.

Kimble, J., and Hirsh, D. (1979). The postembryonic cell lineages of the hermaphrodite and male gonads in *Caenorhabditis elegans*. Dev. Biol. *70*, 396–417.

Kimble, J.E., and White, J.G. (1981). On the control of germ cell development in *Caenorhabditis elegans*. Dev. Biol. *81*, 208–219.

Lee, C.Y., and Baehrecke, E.H. (2001). Steroid regulation of autophagic programmed cell death during development. Development *128*, 1443–1455.

Levine, B., and Yuan, J. (2005). Autophagy in cell death: an innocent convict? J. Clin. Invest. *115*, 2679–2688.

Liu, H., Strauss, T.J., Potts, M.B., and Cameron, S. (2006). Direct regulation of *egl-1* and of programmed cell death by the Hox protein MAB-5 and by CEH-20, a *C. elegans* homolog of Pbx1. Development *133*, 641–650.

Lowe, S.W., Cepero, E., and Evan, G. (2004). Intrinsic tumour suppression. Nature *432*, 307–315.

Lundquist, E.A., Reddien, P.W., Hartwieg, E., Horvitz, H.R., and Bargmann, C.I. (2001). Three *C. elegans* Rac proteins and several alternative Rac regulators control axon guidance, cell migration and apoptotic cell phagocytosis. Development *128*, 4475–4488.

Mangahas, P.M., and Zhou, Z. (2005). Clearance of apoptotic cells in *Caenorhabditis elegans*. Semin. Cell Dev. Biol. *16*, 295–306.

Matsumura, H., Shimizu, Y., Ohsawa, Y., Kawahara, A., Uchiyama, Y., and Nagata, S. (2000). Necrotic death pathway in Fas receptor signaling. J. Cell Biol. *151*, 1247–1256.

Matsuura, A., Tsukada, M., Wada, Y., and Ohsumi, Y. (1997). Apg1p, a novel protein kinase required for the autophagic process in *Saccharomyces cerevisiae*. Gene *192*, 245–250.

Melendez, A., Talloczy, Z., Seaman, M., Eskelinen, E.L., Hall, D.H., and Levine, B. (2003). Autophagy genes are essential for dauer development and life-span extension in *C. elegans*. Science *301*, 1387–1391.

Mello, C.C., Kramer, J.M., Stinchcomb, D., and Ambros, V. (1991). Efficient gene transfer in *C. elegans*: extrachromosomal maintenance and integration of transforming sequences. EMBO J. *10*, 3959–3970.

Metzstein, M.M., Hengartner, M.O., Tsung, N., Ellis, R.E., and Horvitz, H.R. (1996). Transcriptional regulator of programmed cell death encoded by *Caenorhabditis elegans* gene *ces-2*. Nature *382*, 545–547.

Metzstein, M.M., and Horvitz, H.R. (1999). The *C. elegans* cell death specification gene *ces-1* encodes a snail family zinc finger protein. Mol. Cell *4*, 309–319.

Metzstein, M.M., Stanfield, G.M., and Horvitz, H.R. (1998). Genetics of programmed cell death in *C. elegans*: past, present and future. Trends Genet. *14*, 410–416.

Oppenheim, R.W., Flavell, R.A., Vinsant, S., Prevette, D., Kuan, C.Y., and Rakic, P. (2001). Programmed cell death of developing mammalian neurons after genetic deletion of caspases. J. Neurosci. *21*, 4752–4760.

Pasquinelli, A.E., and Ruvkun, G. (2002). Control of developmental timing by micrornas and their targets. Annu. Rev. Cell Dev. Biol. *18*, 495–513.

Pilar, G., and Landmesser, L. (1976). Ultrastructural differences during embryonic cell death in normal and peripherally deprived ciliary ganglia. J. Cell Biol. *68*, 339–356.

Raff, M.C., Whitmore, A.V., and Finn, J.T. (2002). Axonal self-destruction and neurodegeneration. Science *296*, 868–871.

Reinhart, B.J., Slack, F.J., Basson, M., Pasquinelli, A.E., Bettinger, J.C., Rougvie, A.E., Horvitz, H.R., and Ruvkun, G. (2000). The 21-nucleotide *let-7* RNA regulates developmental timing in *Caenorhabditis elegans*. Nature *403*, 901–906.

Roudier, N., Lefebvre, C., and Legouis, R. (2005). CeVPS-27 is an endosomal protein required for the molting and the endocytic trafficking of the low-density lipoprotein receptor-related protein 1 in *Caenorhabditis elegans*. Traffic *6*, 695–705.

Rougvie, A.E., and Ambros, V. (1995). The heterochronic gene *lin-29* encodes a zinc finger protein that controls a terminal differentiation event in *Caenorhabditis elegans*. Development *121*, 2491–2500.

Schulze-Osthoff, K., Krammer, P.H., and Droge, W. (1994). Divergent signalling via APO-1/Fas and the TNF receptor, two homologous molecules involved in physiological cell death. EMBO J. *13*, 4587–4596.

Schumacher, B., Schertel, C., Wittenburg, N., Tuck, S., Mitani, S., Gartner, A., Conradt, B., and Shaham, S. (2005). *C. elegans ced-13* can promote apoptosis and is induced in response to DNA damage. Cell Death Differ. *12*, 153–161.

Shaham, S. (1998). Identification of multiple *Caenorhabditis elegans* caspases and their potential roles in proteolytic cascades. J. Biol. Chem. *273*, 35109–35117.

Siegfried, K., and Kimble, J. (2002). POP-1 controls axis formation during early gonadogenesis in *C. elegans*. Development *129*, 443–453.

Slack, F.J., Basson, M., Liu, Z., Ambros, V., Horvitz, H.R., and Ruvkun, G. (2000). The *lin-41* RBCC gene acts in the *C. elegans* heterochronic pathway between the *let-7* regulatory RNA and the LIN-29 transcription factor. Mol. Cell *5*, 659–669.

Sugimoto, A., Friesen, P.D., and Rothman, J.H. (1994). Baculovirus p35 prevents developmentally programmed cell death and rescues a *ced-9* mutant in the nematode *Caenorhabditis elegans*. EMBO J. *13*, 2023–2028.

Sulston, J.E., Albertson, D.G., and Thomson, J.N. (1980). The *Caenorhabditis elegans* male: postembryonic development of nongonadal structures. Dev. Biol. *78*, 542–576.

Sulston, J.E., and Horvitz, H.R. (1977). Post-embryonic cell lineages of the nematode, *Caenorhabditis elegans*. Dev. Biol. *56*, 110–156.

Sulston, J.E., Schierenberg, E., White, J.G., and Thomson, J.N. (1983). The embryonic cell lineage of the nematode *Caenorhabditis elegans*. Dev. Biol. *100*, 64–119.

Syntichaki, P., Xu, K., Driscoll, M., and Tavernarakis, N. (2002). Specific aspartyl and calpain proteases are required for neurodegeneration in *C. elegans*. Nature *419*, 939–944.

Takacs-Vellai, K., Vellai, T., Puoti, A., Passannante, M., Wicky, C., Streit, A., Kovacs, A.L., and Muller, F. (2005). Inactivation of the autophagy gene *bec-1* triggers apoptotic cell death in *C. elegans*. Curr. Biol. *15*, 1513–1517.

Thellmann, M., Hatzold, J., and Conradt, B. (2003). The Snail-like CES-1 protein of *C. elegans* can block the expression of the BH3-only cell-death activator gene *egl-1* by antagonizing the function of bHLH proteins. Development *130*, 4057–4071.

Timmons, L., and Fire, A. (1998). Specific interference by ingested dsRNA. Nature *395*, 854.

Vercammen, D., Brouckaert, G., Denecker, G., Van de Craen, M., Declercq, W., Fiers, W., and Vandenabeele, P. (1998). Dual signaling of the Fas receptor: initiation of both apoptotic and necrotic cell death pathways. J. Exp. Med. *188*, 919–930.

Vial, J.D. (1958). The early changes in the axoplasm during wallerian degeneration. J. Biophys. Biochem. Cytol. *4*, 551–555.

Vogel, B.E., and Hedgecock, E.M. (2001). Hemicentin, a conserved extracellular member of the immunoglobulin superfamily, organizes epithelial and other cell attachments into oriented line-shaped junctions. Development *128*, 883–894.

Webster, H.D. (1962). Transient, focal accumulation of axonal mitochondria during the early stages of wallerian degeneration. J. Cell Biol. *12*, 361–383.

W.B. Wood, ed. (1988). The Nematode *Caenorhabditis elegans* (Cold Spring Harbor, NY: Cold Spring Harbor Laboratory).

Xu, K., Tavernarakis, N., and Driscoll, M. (2000). Necrotic cell death in *C. elegans* requires the function of calreticulin and regulators of $Ca^{(2+)}$ release from the endoplasmic reticulum. Neuron *31*, 957–971.

Yorimitsu, T., and Klionsky, D.J. (2005). Autophagy: molecular machinery for self-eating. Cell Death Differ. *12* (*Suppl 2*), 1542–1552.

Yuan, J., Shaham, S., Ledoux, S., Ellis, H.M., and Horvitz, H.R. (1993). The *C. elegans* cell death gene *ced-3* encodes a protein similar to mammalian interleukin-1 beta-converting enzyme. Cell *75*, 641–652.

Zhou, Z., Hartwieg, E., and Horvitz, H.R. (2001). CED-1 is a transmembrane receptor that mediates cell corpse engulfment in *C. elegans*. Cell *104*, 43–56.